

KADIR HAS UNIVERSITY
GRADUATE SCHOOL OF SCIENCE AND ENGINEERING



PERFORMANCE OF IEEE 802.11af SYSTEMS UNDER REALISTIC
CHANNEL CONDITIONS

GRADUATE THESIS

MUSTAFA CAN MACİT

May,2016

Mustafa Can Macit

| M.S Thesis |

2016



PERFORMANCE OF IEEE 802.11af SYSTEMS UNDER REALISTIC
CHANNEL CONDITIONS



MUSTAFA CAN MACİT

Submitted to the Graduate School of Science and Engineering in partial fulfillment
of the requirements for the degree of
Master of Science in
Electronics Engineering

KADIR HAS UNIVERSITY

May,2016

“I, Mustafa Can Macit, confirm that the work presented in this thesis is my own. Where information has been derived from other sources, I confirm that this has been indicated in the thesis.”

MUSTAFA CAN MACİT

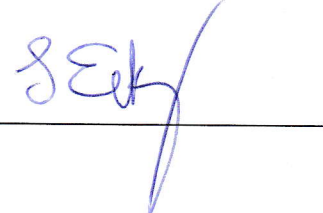
KADIR HAS UNIVERSITY
GRADUATE SCHOOL OF SCIENCE AND ENGINEERING

PERFORMANCE OF IEEE 802.11af SYSTEMS UNDER REALISTIC
CHANNEL CONDITIONS

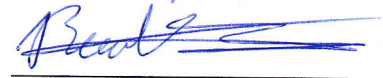
MUSTAFA CAN MACİT

APPROVED BY:

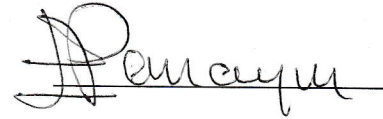
Assoc. Prof. Dr. Serhat Erkuçuk
(Thesis Supervisor)



Asst. Prof. Dr. Tuncer Baykaş



Prof. Dr. Erdal Panayircı



APPROVAL DATE: 31/May/2016

ACKNOWLEDGEMENTS

I would like to thank the following esteemed professors, who have had great impact on my thesis. First, I would like to greatly thank my supervisor, Assoc. Prof. Dr. Serhat Erküçük, not only for his valuable insights and patient guidance to complete the research; but also his academic standing which always inspired me. Without his efforts, this thesis would not be a success. Then, many thanks to my co-supervisor Asst. Prof. Dr. Habib Şenol who is always ready to help whenever I needed with his outstanding knowledge on estimation theory. His guidance helped me throughout the research and writing this thesis. I am deeply grateful to him for the long discussions that helped me sort out the technical details of my work.

I am also grateful to Prof. Dr. Erdal Panayırıcı as the program coordinator for his encouragements. I would like to acknowledge Assoc. Prof. Dr. Serhat Erküçük's research grant from Türk Telekom and Argela under the TT Collaborative Research Awards programme for providing me financial support throughout my graduate studies. I have been a graduate assistant at the Department of Electronics Engineering and a research assistant in Dr. Erküçük's project throughout my studies.

Last, but not the least, I would like to thank my family for their patience, support and confidence in me.

ABSTRACT

Performance of IEEE 802.11af Systems Under Realistic Channel Conditions

As the analog TV broadcasting channels have become less frequently used in the last decade, there has been a great interest in these frequency bands for the deployment of regional, local and personal area networks. Among them, the local area network standard IEEE 802.11af defines PHY and MAC layer implementation of such networks in these unused frequency bands, also named television white space (TVWS). According to the standard, the systems may use contiguous or non-contiguous channels during their operation, depending on the channel availability. Unlike perfectly known channel condition of IEEE 802.11af based systems used in the literature, we investigate in detail the performance of different operation modes of these systems under realistic channel conditions. Accordingly, we implement and compare the performances of perfectly known channel, linear minimum mean-square error (LMMSE) estimator and a matching pursuit (MP) based channel estimator. MP based estimator being the more practical estimator compared to the others, we assess how its performance approaches the other methods. According to simulation results, MP-based channel estimation performance is found to be only 1-2 dB inferior compared to LMMSE-based estimation with known delays in low and medium SNR regions. Also, the effects of guard interval rate, channel resolution and separation of in-between bands in non-contiguous modes are tested in different scenarios. The results of thesis are important for practical implementation of IEEE 802.11af based systems.

ÖZET

IEEE 802.11af Sistemlerinin Gerçek Kanal Koşulları Altındaki Performansı

Analog televizyon yayın kanallarının son 10 yılda daha az sıklıkla kullanılması, bölgesel yerleşimlerinde bu frekans bantlarına büyük ilgi oluşturdu. Bunlar arasında, yerel ağ standardı IEEE 802.11af bu tip kullanılmayan frekans bantları için, bir başka isimle televizyon beyaz boşlukları için fiziksel ve ortam erişim kontrolü katmanlarını tanımlar. Standarda göre sistemler, bitişik veya bitişik olmayan bantları kanal durumuna göre kullanabilir. Literatürdeki mükemmel bilinen kanal koşullarındaki IEEE 802.11af tabanlı sistemlerin aksine, bu tezde gerçek kanal koşulları altında, farklı operasyon modları ayrıntılı incelenmiştir. Buna göre, mükemmel bilinen kanalı, doğrusal minimum ortalama karesel-hata kestirimini ve uyumlu arayış algoritmasını uyguladık ve karşılaştırdık. Uyumlu arayış algoritması tabanlı kestirim, diğerine kıyasla daha pratiktir. Bu algoritmanın performansının, diğer metodlara nasıl yaklaştığı değerlendirilmiştir. Simülasyon sonuçlarına göre, uyumlu arayış algoritması, kanal gecikmesi bilinen doğrusal minimum ortalama karesel-hata kestirim algoritmasıyla karşılaştırıldığında, düşük ve orta işaret-gürültü-oranı bölgelerinde, yalnızca 1-2 dB performans kaybı yaşamaktadır. Bu çalışmada ayrıca koruyucu aralık oranı, kanal çözünürlüğü ve ayrık bantların arasındaki uzaklık gibi parametreler, farklı senaryolar altında test edilmiştir. Tezin sonuçları IEEE 802.11af tabanlı sistemlerin pratik kurulumu için önemlidir.

TABLE OF CONTENTS

ACKNOWLEDGEMENTS	iii
ABSTRACT	iv
ÖZET	v
LIST OF FIGURES	viii
LIST OF TABLES	x
LIST OF SYMBOLS/ABBREVIATIONS	xi
1. INTRODUCTION	1
1.1. Literature Review on TVWS Studies	2
1.2. Motivation of the Thesis	4
1.3. Organisation of the Thesis	5
2. IEEE 802.11af OPERATION IN TV WHITE SPACE	6
2.1. IEEE 802.11 Standards Overview	6
2.2. IEEE 802.11af Overview: Operation Modes	8
2.3. IEEE 802.11af Overview: Subcarriers and Pilot Tones	10
2.4. Related IEEE 802.11af Studies	11
3. SYSTEM MODEL	13
3.1. Transmitter Model	13
3.2. Multipath Channel Model	14
3.3. Receiver Model	16
3.4. Channel Estimation	19
3.4.1. LMMSE Estimator Under Partial Knowledge of Channel State Information	19
3.4.2. Matching Pursuit Based Channel Estimation	20
3.5. Performance Measures	23
4. SIMULATION RESULTS	25
5. CONCLUSIONS and FUTURE RESEARCH	33
5.1. Conclusions	33
5.2. Future Research	34
REFERENCES	35

APPENDIX A: APPENDIX 40
A.1. * 40



LIST OF FIGURES

Figure 2.1.	Coverage of Wireless Standards [29]	6
Figure 2.2.	Illustration of contiguous and non-contiguous operation modes . . .	9
Figure 2.3.	Pilot tone locations for TVHT-MODE-1 and TVHT-MODE-2C . . .	11
Figure 3.1.	Tap coefficients and frequency response of sparse multipath channel	15
Figure 3.2.	Tap coefficients estimation with MP algorithm	22
Figure 4.1.	Average MSE performances in TVHT-MODE-2C for different number of paths when $\rho=8$, GI rate= $\frac{1}{8}$	26
Figure 4.2.	Average MSE performances in TVHT-MODE-2C for different channel resolutions when 3-path wireless channel and GI rate= $\frac{1}{8}$ are used	27
Figure 4.3.	Average MSE performances of TVHT-MODE-2C for various guard interval rates when 3-path wireless channel is considered	28
Figure 4.4.	Average MSE performances in different operation modes when 3-path wireless channel, GI rate= $\frac{1}{8}$ and $\rho = 8$ are used	29
Figure 4.5.	SER comparison of MP algorithm and LMMSE estimation when channel resolution $\rho = 1$, 3-path wireless channel, GI rate= $\frac{1}{8}$ are used	30
Figure 4.6.	SER comparison of MP algorithm and LMMSE estimation when channel resolution $\rho = 4$, 3-path wireless channel, GI rate= $\frac{1}{8}$ are used	31

Figure 4.7. MP algorithm and rounding on LMMSE estimation comparison in
channel resolution $\rho = 8$, 3 path wireless channel, GI rate= $\frac{1}{8}$ 32



LIST OF TABLES

Table 2.1.	Subcarrier index locations [9]	10
Table 4.1.	Simulation parameters for mode TVHT-MODE-2C and TVHT-MODE-2N	25



LIST OF SYMBOLS/ABBREVIATIONS

OFDM	: Orthogonal Frequency Division Multiplexing
AWGN	: Additive white Gaussian noise
TVWS	: Television White Space
BCU	: Basic Channel Unit
IFFT	: Inverse Fast Fourier Transform
PHY	: Physical Layer
MAC	: Medium Access Control
LMMSE	: Linear Minimum Mean Square Error
MP	: Matching Pursuit
UWB	: Ultra Wide Band
WRAN	: Wireless Regional Area Network
WLAN	: Wireless Local Area Network
WPAN	: Wireless Personal Area Network
LAN	: Local Area Network
MAN	: Metropolitan Area Network
SER	: Symbol Error Rate
PER	: Packet Error Rate
FCC	: Federal Communications Commission
ITU-R	: International Telecommunication Union Radiocommunication
ATSC	: Advanced Television Systems Committee
DTV	: Digital television
NTSC	: National Television System Committee
FM	: Frequency Modulation
SNR	: Signal to Noise Ratio
FFT	: Fast Fourier Transform
RMS	: Root Mean Square
ISM	: Industrial Scientific Medical
CCK	: Complementary Code Keying

MSE	: Mean Square Error
CP	: Cyclic Prefix
T_{cp}	: Cyclic Prefix Duration
T_{sym}	: OFDM symbol duration
$s(t)$: Transmitted signal over multipath channel
L	: Number of Multipaths
$\delta(\cdot)$: Kronecker delta function
$\tilde{\tau}_\ell$: Normalized delay of the ℓ th path
α_ℓ	: Tap Coefficient

1. INTRODUCTION

With the advance of digital technology, new communication systems have emerged and occupied the electromagnetic spectrum as licensed systems. In early 2000s, there has been a need for alternative communication systems for better utilization of the spectrum; namely, ultra wideband (UWB) systems [1] and cognitive radios [2]. These systems have been proposed as secondary systems as they have to coexist with licensed primary systems. Accordingly, coexistence mechanisms have been investigated and implemented for peaceful coexistence in the implementation of these systems. Towards the end of 2000s, analog TV bands, mainly the 470-790 MHz band commonly used across the world, have been the main interest of future system designs [3]. Towards the transition from analog to digital TV broadcasting, these TV bands have been unused in many countries. Commonly referred to as TV white space (TVWS), these frequency bands have become popular among telecommunications industry and wireless standardization organizations due to the two main advantageous properties of the band:

1. Better propagation-through-obstacles characteristics of the propagated waves.
2. Longer coverage range for lower cost.

As the regulatory agencies worldwide have decided to eventually open up the unused TVWS for other communication system designs, this has been welcomed by telecommunication companies manufacturing devices ranging from WRAN to WLAN and WPAN devices. Accordingly, within the IEEE LAN/MAN Standards Committee, there have been standardization activities for TVWS communications [4]. This has also led to academic research [5] and to industrial research and development [6] for the feasibility of using the TVWS. In the development of the standards, initially the IEEE 802.22 standard for WRAN has been pursued. The development of the IEEE 802.22 WRAN standard is aimed at using cognitive radio techniques to allow sharing of geographically unused spectrum allocated to the television broadcast service, on a non-interfering basis, to bring broadband access to hard-to-reach, low population density

areas, typical of rural environments, and is therefore timely and has the potential for a wide applicability worldwide [7]. This was the first worldwide attempt to use the TVWS. This has been followed by the WLAN standard IEEE 802.11af [8] and WPAN standard IEEE 802.15.4m [9-11]. IEEE 802.11af standard, also referred to as White-Fi or Super Wi-Fi, is intended for WLAN operation in the TVWS, whereas IEEE 802.15.4m is for low-rate WPAN operation in TVWS. As all these standards consider simultaneous communication in the same TV bands, there has been a coexistence standard, IEEE 802.19.1, also developed that considers peaceful coexistence of different networks as well coexistence with active TV channels [12]. Among TVWS studies, system performance and coexistence are two important topics. The related literature will be presented next.

1.1. Literature Review on TVWS Studies

As for the performance of a newly developed system, the network capacity, coverage area, data rate, symbol-error rate (SER) and packet-error rate (PER) performances are important factors that define the new system properties. For the performance assessment of a TVWS device, first of all, the capacity in TVWS should be determined. In [13], the authors consider the Federal Communications Commission's (FCC) database of television transmitters, USA census data from 2000, and standard wireless propagation and information-theoretic capacity to see the distribution of data-rates available for wireless Internet. They point out that rural area customers could enjoy higher data rates compared to urban area customers. A similar study was conducted for Europe in [14] and [15]. Considering 11 European countries and adopting the (International Telecommunication Union Radiocommunication) ITU-R's statistical channel model, the authors confirm that the availability of white spaces in Europe in the 470-790 MHz band is notably less than in the USA. In [16], the authors are motivated by the importance of the need to reliably detect incumbent licensed systems (Advanced Television Systems Committee for Digital Television (ATSC DTV) signals, National Television System Committee (NTSC) analog TV signals and FM wireless microphone signals) operating in TVWS in North America. They present spectrum sensing algorithms for these primary systems and present the detection performance results. They

claim to reliably determine the availability of a TV channel when the signal-to-noise-ratio (SNR) is even -18dB. In [17], the authors conduct a measurement campaign to assess the accuracy of three widely used propagation models in predicting TV signal strengths for configurations of multiple high-power transmitters. The results are used in improving coverage prediction for primary multi-transmitter networks operating in TVWS. In [18], the authors present a quantitative analysis of the performance of a network of Wi-Fi-like access points operating in TVWS in order to obtain a realistic estimate of achievable range and downlink rate of such a secondary system. In [19], the authors study the database-assisted distributed white-space access point network design to achieve robustness against the secondary users dynamically entering and leaving the system. In [20], an overview of physical layers of ECMA-392 standard and IEEE 802.11af standard are presented, followed by packet-error rate comparison. The effects of different numbers of FFT size, RMS delay spread, and channel bandwidths are discussed through simulations. In [21], the authors consider region-based mobility procedure and formulate an achievable throughput in terms of the average number of available channels, the effective data transmission time, and the TV band database fees. In [22], the authors present a new channel assignment algorithm that performs controlled channel sharing among neighboring access points. They also apply this algorithm as a modified 802.22 MAC layer protocol. In [23], the authors consider the deployment of a cellular network in TVWS and assess the performance in Germany with high urban densities and inherent cross-border dependencies. The results show that although significant amounts of secondary spectrum may exist, they cannot be efficiently exploited by low-density network deployments. In [24], the authors propose a dynamic frequency selection technique for WLANs operating in TVWS. Compared to conventional dynamic frequency selection, the total time consumption is reduced by 40 % with the proposed technique.

As for the peaceful coexistence of this system, its effect on primary users (i.e., active TV broadcasting) and other secondary networks (and vice versa, the effect of other users on the new device) is important and should be carefully investigated. Coexistence between future independent networks (c.f. WLAN, WRAN, etc.) in the TVWS is essential in order to provide a high-level of quality-of-service to end users. Consequently,

the IEEE 802 LAN/MAN standards committee has approved the 802.19.1 standardization project to specify radio-technology-independent methods for coexistence among dissimilar or independently operated wireless devices and networks [12]. In [25], the authors (most of them are members of the IEEE802.19.1 task group) provide a detailed overview of the regulatory status of TVWS in the USA and Europe, analyze the coexistence problem in TVWS, and summarize existing coexisting mechanisms to improve coexistence in TVWS. In [26], the authors present the performance evaluation of the IEEE 802.19.1 coexistence system based on simulation. They consider both coexistence (i.e., using the discovery service of IEEE 802.19.1 system) and non-coexistence (i.e., determining the neighbors by themselves) simulation scenarios and present the percentages of white space devices operating in the presence of neighboring devices. In [27], the authors address the problem of coexistence among wireless networks in TVWS. They present a standard independent framework to enable exchange of information relevant for coexistence based on two mechanisms: centralized and distributed. Then, they present spectral availability results for various household entities of two scenarios (depending on information exchange being available or not). In [28], the authors exploit Wi-Fi white space for ZigBee performance assurance. They characterize the white space in Wi-Fi traffic, analyze the performance of a ZigBee link in the presence of Wi-Fi interference and develop a new ZigBee frame control protocol. The above summarized studies [25-28] mainly consider the coexistence issue independent from radio-specific modulations and implementations.

1.2. Motivation of the Thesis

In this thesis, physical layer performance analysis of the WLAN standard in TVWS, IEEE 802.11af, is the main interest, among the WRAN, WLAN and WPAN standards mentioned above. In physical layer design, current literature on IEEE 802.11af standard assumes that channel parameters are known by the receiver and all simulations are performed with respect to known parameters without channel estimation. However, channel estimation would be needed before data transmission for practical implementation. Two main aspects should be explored.

1. How would a realistic channel estimation approach perform with respect to ideal channel?
2. How would the non-contiguous operation bands affect the channel estimation performance?

The effect of channel estimation on different operation modes of the IEEE 802.11af standard, which will be defined in next chapter, is studied and simulations are performed under different channel resolution values, different number of paths and different guard interval rates. Results are compared with the performance under perfect knowledge of the channel. Performance results can be useful and may serve as a guide for physical layer design of IEEE 802.11af devices.

1.3. Organisation of the Thesis

This thesis is organised as follows:

- Chapter 2 will provide an overview of the IEEE 802.11af standard and the related literature.
- Chapter 3 will explain the mathematical model of the system, including the transmitter, receiver and channel models as well as the channel estimation methods.
- Chapter 4 will present the simulation results and discuss the effects of different system design parameters.
- Finally, Chapter 5 will present the concluding remarks and will discuss possible extensions of the research.

2. IEEE 802.11af OPERATION IN TV WHITE SPACE

In this chapter, a short overview of IEEE 802.11 based standards will be provided followed by explaining the operation modes and pilot tones of IEEE 802.11af standard. Finally, related studies on system performance of IEEE 802.11af will be given.

2.1. IEEE 802.11 Standards Overview

Wireless network standards are being developed since 1997 by the Institute of Electrical and Electronics Engineers (IEEE). General name of these network standards in WLAN is “IEEE 802.11”, which represents the technical requirements that should be obeyed when building up a communication system in a local area network. As a result of high demand for IEEE 802.11 type applications, Wi-Fi has spread in our lives incredibly fast. These IEEE 802.11 based standards make it possible for people to use their laptop computers in many places, using a wireless link rather than a cable.

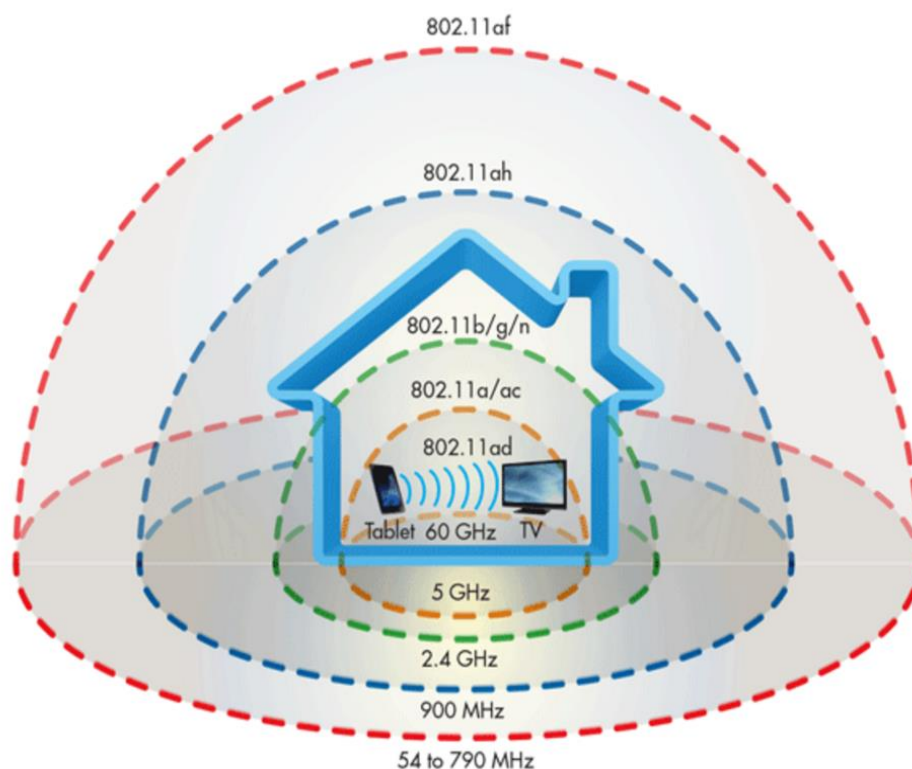


Figure 2.1. Coverage of Wireless Standards [29]

Depending on different spectrum usage requirements, various IEEE 802.11 standards have been made. In Fig 2.1, different members of the IEEE 802.11 family are shown. Among these standards, 802.11ad operates at the 60 GHz band and it has the smallest coverage area. In the order of coverage from small to large, 802.11a and 802.11ac standards are developed at the 5 GHz band, 802.11b/g/n standards operate at the 2.4 GHz band, 802.11ah is designed for the 900 MHz band and 802.11af standard which has the largest coverage area operates in the 54-790 MHz band. In the following, further details of IEEE 802.11 based standards are provided.

- **IEEE 802.11a:** Wireless network that operates in 5 GHz industrial, scientific and medical (ISM) band with data rates up to 54 Mbps, which has up to 20 MHz channel bandwidth. Orthogonal frequency division multiplexing (OFDM) signal of 802.11a contains 64 subcarriers, 48 of them is used for data transmission, 4 of them is reserved for pilot symbols and 12 of them are used as null.
- **IEEE 802.11b:** Wireless network that operates in 2.4 GHz ISM band with data rates up to 11 Mbps, which has 20 MHz bandwidth and uses Complementary Code Keying (CCK) modulation.
- **IEEE 802.11n:** Wireless network that operates in both 2.4 GHz and 5 GHz ISM band with data rates up to 600 Mbps, which have 2 different bandwidths, 20 MHz and 40 MHz. 64 subcarriers are determined for 20 MHz bandwidth mode and 4 pilot symbols are inserted in subcarriers. 128 subcarriers are determined for 40 MHz bandwidth mode and 6 pilot symbols are inserted in subcarriers.
- **IEEE 802.11ac:** Wireless network that operates in 5.8 GHz unlicensed band with data rates up to 6.93 Gbps, which have 20, 40 and 80 MHz bandwidth for mandatory mode, 160 MHz bandwidth for optional mode.
- **IEEE 802.11ad:** Wireless network that operates in 60 GHz ISM band with data rates up to 7 Gbps, which uses beamforming technology. Typical distance of IEEE 802.11ad systems are 1-10 meter.
- **IEEE 802.11af:** Wireless network that operates in TV white space spectrum. More details about IEEE 802.11af systems are provided in the following subsections. Among important properties of IEEE 802.11af systems, operation modes and pilot tones are focused on and presented next.

2.2. IEEE 802.11af Overview: Operation Modes

Among WRAN, WLAN, WPAN standardization activities, IEEE 802.11af standard defines the physical (PHY) and medium access control (MAC) layers for WLAN operation in TVWS.

In order to achieve high data rates, TV High Throughput (TVHT) PHY has been defined in the standard [9]. Accordingly, the data transmission is based on OFDM systems, where the systems are named basic channel units (BCU) having a bandwidth of 6 MHz, 7 MHz or 8 MHz, depending on the regulatory domain. Since the TVWS for the standard is considered as the 54-806 MHz bandwidth, for a BCU bandwidth of 6 MHz in US, there are 67 non-overlapping BCUs (54-72 MHz, 76-88 MHz, 174-216 MHz, 470-608 MHz, and 614806 MHz) [30]. While the IEEE 802.11af based devices have to support the mandatory transmission mode of one BCU (represented with TVHT-MODE-1), optional transmission modes use multi-BCUs and may achieve higher data rates.

There are four optional modes defined in the standard [9]:

- 1) Two contiguous BCUs (TVHT-MODE-2C)
- 2) Two non-contiguous BCUs (TVHT-MODE-2N)
- 3) Four contiguous BCUs (TVHT-MODE-4C)
- 4) Two non-contiguous frequency segments, each of which comprising two contiguous BCUs (TVHT-MODE-4N)

While an IEEE 802.11af based device may operate on contiguous BCUs (TVHT-MODE-2C and TVHT-MODE-4C) and increase its transmission bandwidth, depending on the unavailability of contiguous BCUs it may operate in the non-contiguous modes (TVHT-MODE-2N and TVHT-MODE-4N). Operation modes of two contiguous and non-contiguous BCUs are illustrated in Fig 2.2. In the non-contiguous operation mode,

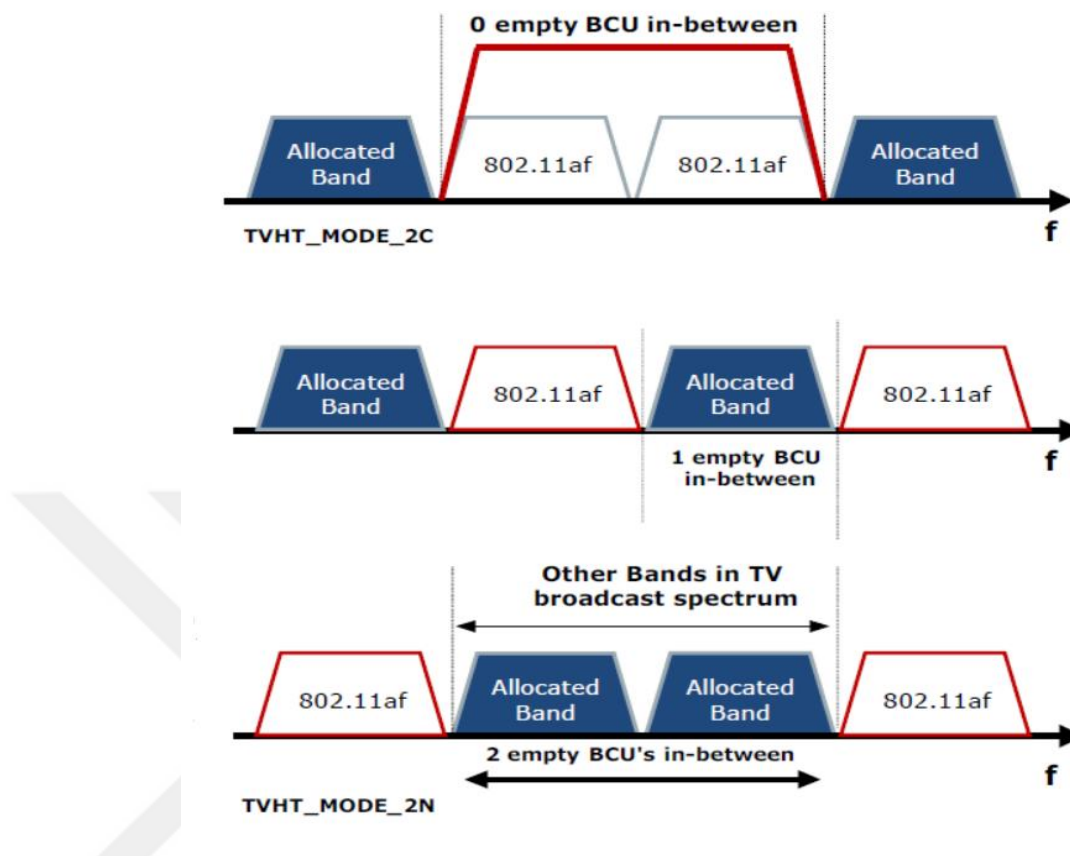


Figure 2.2. Illustration of contiguous and non-contiguous operation modes

the data subcarriers in the unused frequency bands can be nulled and the system complexity can be comparable to the contiguous mode. Furthermore, under the perfectly estimated channel condition, system performances are similar. However, in practice the frequency selective nature of the channel and the use of limited number of pilot tones (6 for the mandatory mode) are expected to degrade the channel estimation performance as the separation between the non-contiguous BCUs is increased. This effect will be investigated considering the system design parameters defined in the standard and for practical channel models.

In this study, system performances will be assessed for TVHT-MODE-2C and TVHT-MODE-2N in the subsequent chapters. These two modes are selected to observe the effect of band separation for the same bandwidth and data rate. In the TVHT-MODE-2C, data transmission bandwidth is 12 MHz, given that each BCU has a 6 MHz bandwidth. However, depending on channel availability, TVHT-MODE-2N can be an alternative mode. It will consist of two non-contiguous 6+6 MHz bandwidth. In the following chapters, effect of band separation on the system performance will be discussed.

2.3. IEEE 802.11af Overview: Subcarriers and Pilot Tones

One of the most important issues in designing the mathematical model of this system is subcarrier and pilot tone locations. Pilot tone numbers and locations have a direct effect on estimating channel tap coefficients, which is important for performance of the system.

Parameteres	TVHT-MODE-2C	TVHT-MODE-2N
Total Subcarriers(N)	288	288
Active Subcarriers(N_A)	256	256
Total number of occupied subcarriers across all BCU's(N_{TT})	228	228
Subcarrier Index	(-130 to -74 , -70 to -14, +14 to 70, +74 to 130)	(-58 to -2, +2 to 58 for each BCU)

Table 2.1. Subcarier index locations [9]

In Table 2.1, active subcarrier numbers and their index values are given for OFDM signal generation. Both TVHT-MODE-2C and TVHT-MODE-2N have 6 MHz bandwidth for each BCU with inserted 144 subcarriers, 108 of them are for data transmission, 6 of them are for pilot symbols and 30 of them are for nulling operation. Considering subcarrier numbers and bandwidth, subcarrier spacing (Δf) can be found as $\frac{6}{144}$ MHz = $41\frac{2}{3}$ KHz.

In Fig. 2.3, inserted pilot tones are illustrated for TVHT-MODE-1 and TVHT-MODE-2C. According to [9], for TVHT-MODE-1, six pilot tones should be inserted in subcarriers at index values $\{-53, -25, -11, 11, 25, 53\}$. When multiple BCUs are used (TVHT-MODE-2C, TVHT-MODE-2N, TVHT-MODE-4C, and TVHT-MODE-4N), each BCU should use the same pilot tone locations, however their corresponding index values will be different.

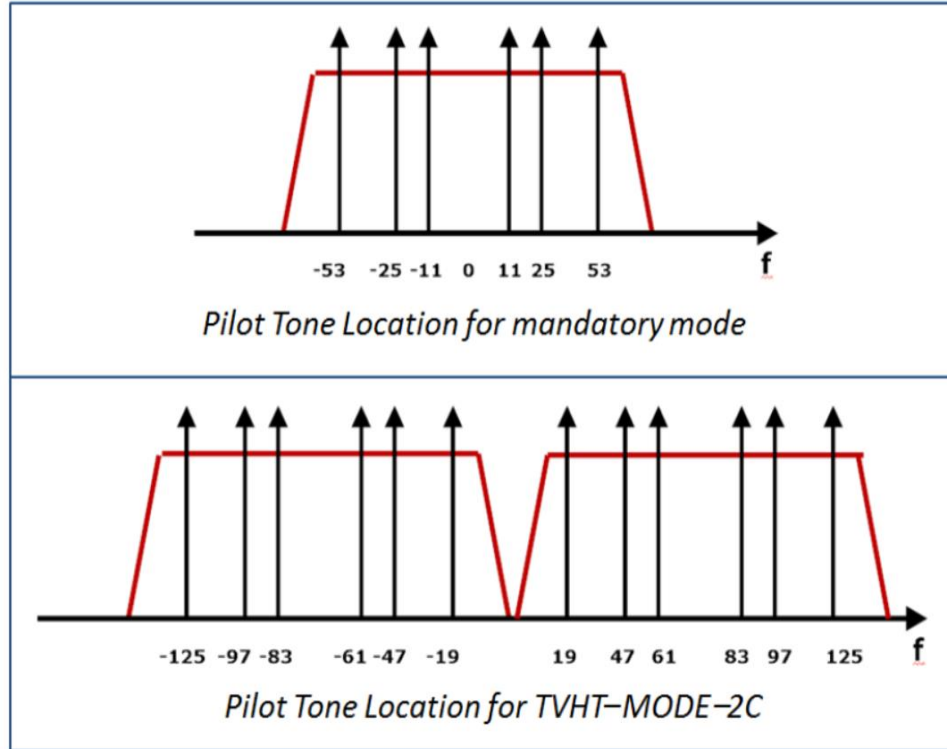


Figure 2.3. Pilot tone locations for TVHT-MODE-1 and TVHT-MODE-2C

2.4. Related IEEE 802.11af Studies

Considering the IEEE 802.11af standard, following studies have been conducted on the system performance. However, these studies do not evaluate the system performance with a realistic channel estimation algorithm that considers operation modes, subcarrier and pilot tone locations of the standard.

In [31], the authors present the first ever prototype built based on the IEEE 802.11af standard considering both PHY and MAC layer aspects. The performance of PHY layer channel bounding is compared with MAC layer channel aggregation in terms of data rates and packet error rates in [32]. The performance of an IEEE 802.11af based network is analyzed considering the effects of inter-access point interference and congestion in [33]. The performances of IEEE 802.11af, IEEE 802.22 and IEEE 802.15.4m

are assessed while they are in close proximity, in order to determine tolerable interference levels in [34]. Packet error rate performances of IEEE 802.11af standard and the similar local area network standard ECMA-392 are compared considering the system parameters defined in the standards in [35]. In [36], a partial subcarrier system for the IEEE 802.11af systems is proposed to effectively use the TVWS and increase the throughput. While evaluating the system performances in [31]–[35], the simple operation mode of an IEEE 802.11af system that uses a single frequency band is considered. However, these systems may use multiple available channels, which may be contiguous or non-contiguous. In [36], the different operation modes are considered, however, the performances provided did not include the effects of channel estimation.

In order to determine the realistic performance of an IEEE 802.11af based system, the system model will be presented next.

3. SYSTEM MODEL

In this chapter, mathematical models of the transmitter, multipath channel and receiver are presented in detail, followed by the two channel estimation methods.

3.1. Transmitter Model

We consider a zero padded OFDM system with N subcarriers employing actively K subcarriers to transmit data symbols, and nothing is transmitted from the remaining $N-K$ carriers for the purpose of zero-padding. During any OFDM symbol, each active subcarrier is modulated by a data symbol $d_m[k]$, where m and k represent the OFDM symbol index and the discrete subcarrier frequency, respectively. After taking a K -point inverse fast Fourier transform (IFFT) of the data sequence and adding a cyclic prefix (CP) of duration T_{cp} before transmission to eliminate inter-symbol interference, the transmitted continuous time-domain complex valued signal can be expressed as

$$s(t) = \frac{1}{N} \sum_{m=0}^{M-1} \sum_{k=-K/2}^{K/2-1} d_m[k] e^{j2\pi k \Delta f (t - mT_{sym} - T_{cp})} \zeta(t - mT_{sym}), \quad (3.1)$$

where $\Delta f = 1/T$ is the OFDM subcarrier spacing, T stands for OFDM symbol duration, $T_{sym} = T + T_{cp}$ is the duration of an entire OFDM symbol, M is the OFDM block length, and $\zeta(t)$ denotes the unit pulse given by

$$\zeta(t) = \begin{cases} 1 & , \quad 0 \leq t \leq T_{sym} \\ 0 & , \quad \text{otherwise.} \end{cases} \quad (3.2)$$

3.2. Multipath Channel Model

The signal $s(t)$, is transmitted over a wireless multipath channel with impulse response given by [38]

$$h(t) = \sum_{\ell=0}^{L-1} \alpha_{\ell} \delta(t - \tau_{\ell}) , \quad (3.3)$$

where L shows the number of channel paths, $\delta(\cdot)$ denotes the Kronecker delta function, α_{ℓ} is the multipath gain and τ_{ℓ} is the delay of the ℓ th path. Path gains, $\{\alpha_{\ell}\}_{\ell=0}^{L-1}$, are considered independent from each other and assumed to be zero-mean complex Gaussian random variables. They have the normalized powers, $\{\Omega_{\ell}\}_{\ell=0}^{L-1}$, which obey an exponentially decaying power delay profile, $\Omega_{\ell} = C e^{-\tau_{\ell}/T_{cp}}$, where C is the power normalization constant such that $\sum_{\ell=0}^{L-1} \Omega_{\ell} = 1$. The channel delays, $\{\tau_{\ell}\}_{\ell=0}^{L-1}$, are independent with respect to each other and uniformly distributed within the interval $[0, T_{cp}]$.

In Figure 3.1, tap coefficients and their frequency responses are represented. The 2-path and 3-path channels with cyclic prefix duration chosen as $1/8$ of the symbol duration is given in this snapshot.

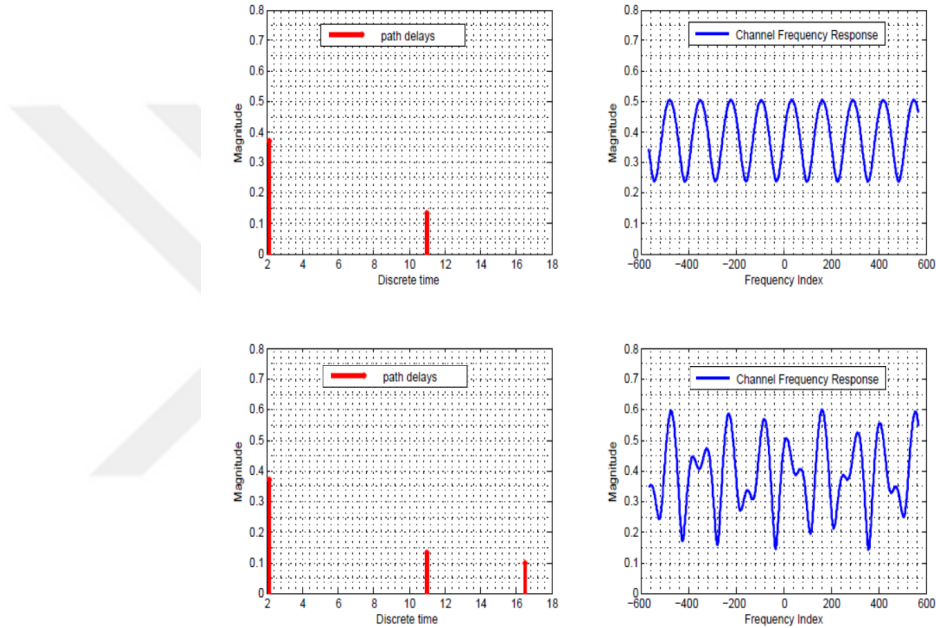


Figure 3.1. Tap coefficients and frequency response of sparse multipath channel

In the following, receiver model of the system will be presented, where estimation of delays and gains will be explained in detail. Additionally, performance measures and how they can be calculated will be given.

3.3. Receiver Model

The time domain received signal can be obtained as

$$\begin{aligned}
y(t) &= \sum_{\ell=0}^{L-1} \alpha_{\ell} s(t - \tau_{\ell}) + w(t) \\
&= \frac{1}{N} \sum_{\ell=0}^{L-1} \sum_{m=0}^{M-1} \sum_{k=-K/2}^{K/2-1} \alpha_{\ell} d_m[k] e^{j \frac{2\pi k}{T} (t - \tau_{\ell} - mT_{sym} - T_{cp})} \\
&\quad \times \zeta(t - \tau_{\ell} - mT_{sym}) + w(t) ,
\end{aligned} \tag{3.4}$$

where $w(t)$ is zero-mean complex additive white Gaussian noise (AWGN).

At the receiver, $y(t)$ is converted into the discrete-time signal by means of low-pass filtering and A/D conversion with the sampling interval $T_s = T/N$. Assuming that K active subcarriers are within the region of frequency response of both transmitter and receiver filters, and the number of channel paths and the path delays do not change during M OFDM symbol duration, it is sufficient to consider the channel estimation within M OFDM symbol block. Therefore, the n th time sample within m th OFDM symbol after the CP removal can be expressed as

$$\begin{aligned}
y_m[n] &= y(mT_{sym} + T_{cp} + nT_s) , \quad n = 0, 1, \dots, (N - 1) \\
&= \frac{1}{N} \sum_{\ell=0}^{L-1} \sum_{k=-K/2}^{K/2-1} \alpha_{\ell} d_m[k] e^{j \frac{2\pi k}{N} (n - \check{\tau}_{\ell})} + w_m[n] ,
\end{aligned} \tag{3.5}$$

where $\check{\tau}_{\ell} = \tau_{\ell}/T_s$ is the normalized delay of the ℓ th path and $w_m[n] = w(mT_{sym} + T_{cp} + nT_s)$ denotes the AWGN sample at time n within m th OFDM symbol duration.

An N -point Fast Fourier Transform (FFT) is applied to transform the sequence $y_m[n]$ into frequency domain. The output at subcarrier k during m th OFDM symbol

can be represented by

$$\begin{aligned}
Y_m[k] &= \sum_{n=0}^{N-1} y_m[n] e^{-j\frac{2\pi}{N}nk}, \quad -\frac{K}{2} \leq k \leq \left(\frac{K}{2} - 1\right) \\
&= \sum_{\ell=0}^{L-1} \alpha_\ell d_m[k] e^{-j\frac{2\pi k}{N}\check{\tau}_\ell} + W_m[k], \quad (3.6)
\end{aligned}$$

where $W_m[k] \sim \mathcal{CN}(0, N_0)$. It is straightforward that the vector form of (3.6) can be expressed as

$$\mathbf{Y}_m = \sum_{\ell=0}^{L-1} \mathbf{a}_m(\check{\tau}_\ell) \alpha_\ell + \mathbf{W}_m, \quad (3.7)$$

where

$$\begin{aligned}
\mathbf{Y}_m &= \left[Y_m\left[-\frac{K}{2}\right], Y_m\left[-\frac{K}{2}+1\right], \dots, Y_m\left[\frac{K}{2}-1\right] \right]^T \\
\mathbf{W}_m &= \left[W_m\left[-\frac{K}{2}\right], W_m\left[-\frac{K}{2}+1\right], \dots, W_m\left[\frac{K}{2}-1\right] \right]^T \\
\mathbf{a}_m(\check{\tau}_\ell) &= \mathbf{d}_m \odot \boldsymbol{\nu}(\check{\tau}_\ell) \\
\mathbf{d}_m &= \left[d_m\left[-\frac{K}{2}\right], d_m\left[-\frac{K}{2}+1\right], \dots, d_m\left[\frac{K}{2}-1\right] \right]^T, \quad (3.8)
\end{aligned}$$

$\boldsymbol{\nu}(\check{\tau}_\ell)$ is a column vector with entries $e^{-j\frac{2\pi k}{N}\check{\tau}_\ell}$, $(\cdot)^T$ denotes the transpose operator and \odot stands for the Hadamard product. Stacking vectors in (3.7), we can rewrite the observation model as

$$\mathbf{Y} = \sum_{\ell=0}^{L-1} \mathbf{a}(\check{\tau}_\ell) \alpha_\ell + \mathbf{W}, \quad (3.9)$$

where

$$\begin{aligned}
\mathbf{Y} &= \left[\mathbf{Y}_0^T, \mathbf{Y}_1^T, \dots, \mathbf{Y}_{(M-1)}^T \right]^T \\
\mathbf{a}(\check{\tau}_\ell) &= \left[\mathbf{a}_0^T(\check{\tau}_\ell), \mathbf{a}_1^T(\check{\tau}_\ell), \dots, \mathbf{a}_{(M-1)}^T(\check{\tau}_\ell) \right]^T \\
\mathbf{W} &= \left[\mathbf{W}_0^T, \mathbf{W}_1^T, \dots, \mathbf{W}_{(M-1)}^T \right]^T, \quad (3.10)
\end{aligned}$$

In this work, we are mainly interested in estimation of sparse multipath channel based on the observation (3.9). The overall continuous-time channel impulse response is represented by a parametric model in which the ℓ th distinct path is characterized by path delay, $\check{\tau}_\ell$, and tap coefficient, α_ℓ . In practice, the sparsity assumption does not always hold due to the non-integer normalized path delays in the equivalent discrete-time baseband representation of the channel. Therefore, such an estimated channel may differ substantially from the original channel. To achieve a better channel estimation performance, the A/D conversion at the input of the OFDM receiver is implemented with a sampling period T_s/ρ , $\rho \in \{1, 2^1, 2^2, \dots\}$ leading to a finer delay resolution. Consequently, the continuous-valued normalized path delays $\check{\tau}_\ell, \ell \in \{0, 1, \dots, (L-1)\}$ can be discretized as $\eta_\ell = \lfloor \frac{\check{\tau}_\ell}{T_s/\rho} \rfloor = \lfloor \rho \check{\tau}_\ell \rfloor$ and take values from the set of possible discrete path delays

$$\eta_\ell \in \{0, 1, \dots, (\rho L_{cp} - 1)\}, \quad (3.11)$$

where $L_{cp} = \lfloor T_{cp}/T_s \rfloor$, and $\lfloor \cdot \rfloor$ denotes the floor operator. Based on the associated discrete random channel tap positions $\{\eta_\ell\}_{\ell=0}^{L-1}$, the received signal in (3.9) can be rewritten as

$$\mathbf{Y} = \sum_{\ell=0}^{L-1} \mathbf{a}_{\eta_\ell} \alpha_\ell + \mathbf{W} = \mathbf{A} \tilde{\boldsymbol{\alpha}} + \mathbf{W}, \quad (3.12)$$

where $\mathbf{a}_{\eta_\ell} = \mathbf{a}(\check{\tau}_\ell)|_{\check{\tau}_\ell = \eta_\ell/\rho}$ is the η_ℓ th column vector of the so-called *dictionary matrix* $\mathbf{A} = [\mathbf{a}_0, \mathbf{a}_1, \dots, \mathbf{a}_{(\rho L_{cp}-1)}] \in \mathcal{C}^{MK \times \rho L_{cp}}$. Vector $\tilde{\boldsymbol{\alpha}}$ is the sparse multipath tap coefficient vector with unknown non-zero elements $\{\alpha_\ell\}_{\ell=0}^{L-1}$ at unknown tap positions, $\{\eta_\ell\}_{\ell=0}^{L-1}$. The estimation problem of non-zero elements of the sparse multipath tap coefficient vector $\tilde{\boldsymbol{\alpha}}$ and tap positions in (3.12) can be solved by sparse signal recovery methods. For data detection, it is straightforward that the observation equation in (3.6) can be rewritten as

$$Y_m[k] = H[k] d_m[k] + W_m[k], \quad (3.13)$$

where $H[k] = \sum_{\ell=0}^{L-1} \alpha_{\ell} e^{-j \frac{2\pi k}{\rho N} \eta_{\ell}}$ is the frequency domain channel response at discrete frequency k .

3.4. Channel Estimation

In this section LMMSE estimation under partial knowledge of channel state information and MP based channel estimation are explained. It is assumed that tap delay locations are known and rounded to the nearest channel resolution for LMMSE based channel estimation. Therefore, LMMSE estimator estimates only tap coefficients. On the other hand, MP algorithm estimates both tap delay locations and tap coefficients. More details about these two estimation techniques can be found in Sections 3.4.1 and 3.4.2.

3.4.1. LMMSE Estimator Under Partial Knowledge of Channel State Information

Under the assumption of known $\{\check{\tau}_{\ell}\}_{\ell=0}^{L-1}$ for the perfect knowledge tap positions or known $\{\eta_{\ell}\}_{\ell=0}^{L-1}$ for the knowledge of tap positions at the nearest integer multiple of T_s/ρ , we employ the LMMSE estimator to estimate the nonsparse tap coefficient vector $\boldsymbol{\alpha} = [\alpha_0, \alpha_1, \dots, \alpha_{(L-1)}]^T$. While applying the LMMSE estimator using (3.12), in order to obtain the dictionary matrix with column vectors $\{\mathbf{a}(\check{\tau}_{\ell})\}_{\ell=0}^{L-1}$ or $\{\mathbf{a}_{\eta_{\ell}}\}_{\ell=0}^{L-1}$ assuming perfect knowledge or the knowledge at the nearest integer multiple of T_s/ρ tap delay position, respectively, we use the pilot symbols in their respective positions and set the unknown data symbols to zero [37]. With the channel tap delay position knowledge, using the observation equation in (3.12), the LMMSE estimator of $\boldsymbol{\alpha}$ can be given as

$$\hat{\boldsymbol{\alpha}} = (\mathbf{A}^{(p)\dagger} \mathbf{A}^{(p)} + N_0 \boldsymbol{\Omega}^{-1})^{-1} \mathbf{A}^{(p)\dagger} \mathbf{Y}^{(p)}, \quad (3.14)$$

where $(\cdot)^{\dagger}$ denotes the complex conjugate transpose operator, $\mathbf{Y}^{(p)}$ is the frequency domain receive vector having elements at pilot subcarriers and $\boldsymbol{\Omega}$ represents the diagonal covariance matrix of the nonsparse tap coefficient vector $\boldsymbol{\alpha}$. The covariance matrix $\boldsymbol{\Omega}$

has the main diagonal elements $\{\Omega_\ell\}_{\ell=0}^{L-1}$ that are determined with respect to tap delay positions. The dictionary matrix $\mathbf{A}^{(p)}$ can be obtained as $\mathbf{A}^{(p)} = [\mathbf{a}^{(p)}(\check{\tau}_0), \mathbf{a}^{(p)}(\check{\tau}_1), \dots, \mathbf{a}^{(p)}(\check{\tau}_{(L-1)})]$ or $\mathbf{A}^{(p)} = [\mathbf{a}_{\eta_0}^{(p)}, \mathbf{a}_{\eta_1}^{(p)}, \dots, \mathbf{a}_{\eta_{(L-1)}}^{(p)}]$ while assuming perfect knowledge or the knowledge at the nearest integer multiple of T_s/ρ tap delay position, respectively.

3.4.2. Matching Pursuit Based Channel Estimation

Matching Pursuit (MP) is a greedy algorithm, which can be used for sparse channel estimation. It can estimate both tap delay positions and tap coefficients. Due to this feature, it can be use for real and practical implementations.

Using the dictionary matrix \mathbf{A} in (3.12), $\mathbf{A}^{(p)}$ can be obtained as $\mathbf{A}^{(p)} = [\mathbf{a}_{\eta_0}^{(p)}, \mathbf{a}_{\eta_1}^{(p)}, \dots, \mathbf{a}_{\eta_{(L-1)}}^{(p)}]$, where $\mathbf{A}^{(p)}$ has elements only at the pilot subcarrier locations and N_p is the number of pilot tones.

First step of MP is to generate proxy data. Residual vector, which is equivalent to pilot locations at the observed vector $\mathbf{Y}^{(p)}$, is updated in every iteration by η , which is the index value at the maximum proxy value. Algorithm repeats until break condition occurs.

To achieve a robust MP performance, ϵ is defined for break condition. The MP Algorithm is given below.

Data: $\mathbf{Y}^{(p)}, \mathbf{A}^{(p)}$

Define: ϵ

Initialize: $\hat{\alpha} = 0, \ell = 1$

while $\ell \leq N_p$ **do**

$$\hat{\eta}_\ell = \arg \max_{\eta_\ell} \frac{|\mathbf{a}_{\eta_\ell}^H \mathbf{r}_{\ell-1}|^2}{\|\mathbf{a}_{\eta_\ell}\|^2}, \eta_\ell = 1, \dots, \rho N_{cp} \text{ and } \eta_\ell \notin \{ \hat{\eta}_{\ell_1}, \dots, \hat{\eta}_{\ell-1} \}$$

$$\hat{\alpha}_{\hat{\eta}_\ell} = \frac{\mathbf{a}_{\hat{\eta}_\ell}^H \mathbf{r}_{\ell-1}}{\|\mathbf{a}_{\hat{\eta}_\ell}\|^2}$$

$$\mathbf{r}_\ell = \mathbf{r}_{\ell-1} - \mathbf{a}_{\hat{\eta}_\ell} \hat{\alpha}_{\hat{\eta}_\ell}$$

$$\ell = \ell + 1$$

if $|\hat{\alpha}_{\hat{\eta}_\ell}| < \epsilon \times \sqrt{\sum_{\ell'=0}^{\ell} |\hat{\alpha}_{\ell'}|^2}$ **then**

break;

else

end

end

Result: $\hat{\eta}, \hat{\alpha}$

Algorithm 1: Matching Pursuit Algorithm

The result of the algorithm represents $\hat{\eta}$ and $\hat{\alpha}$ which are the estimated tap delay locations and tap coefficients, respectively.

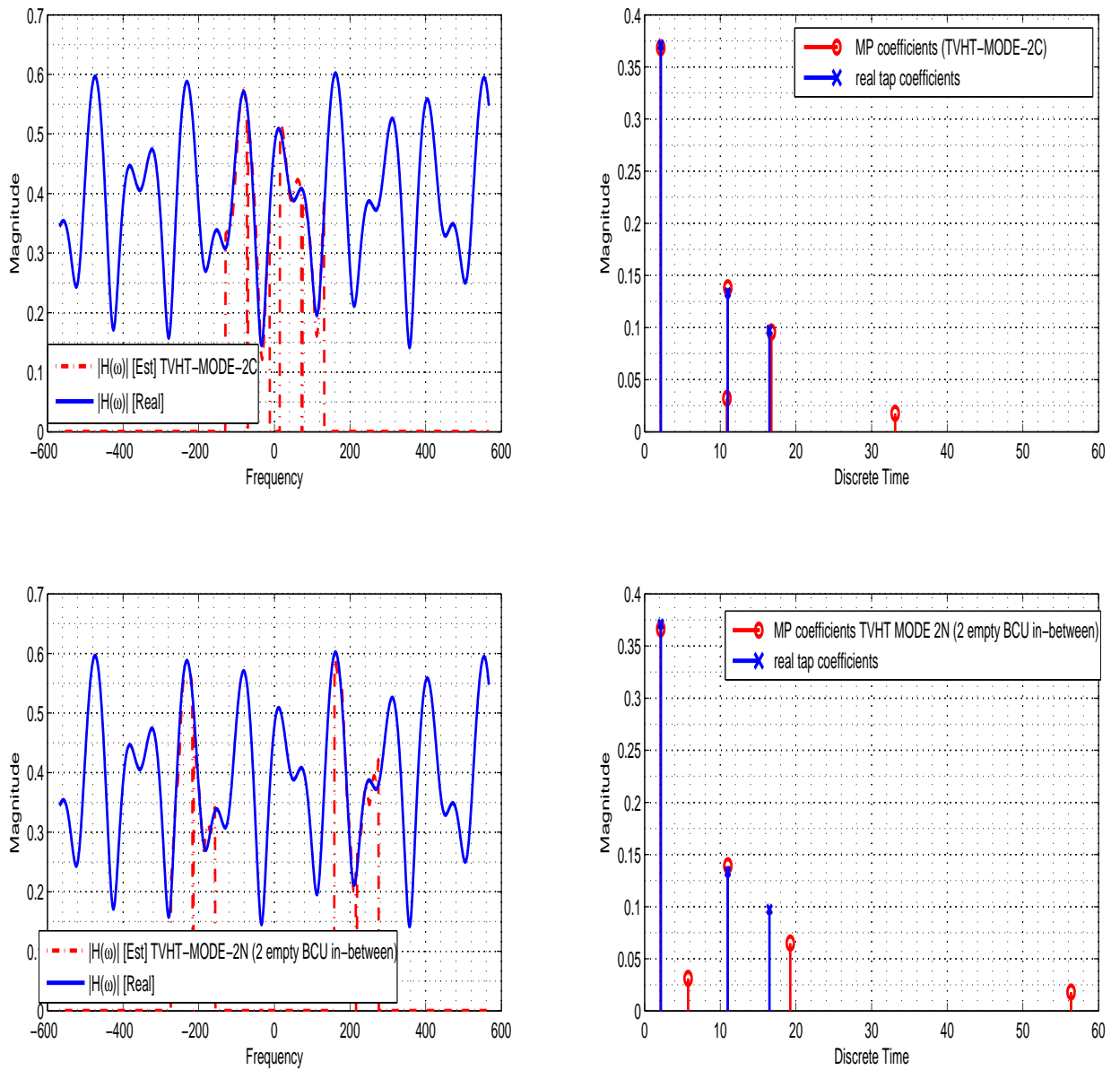


Figure 3.2. Tap coefficients estimation with MP algorithm

There are several issues that can affect the estimation performance of the MP algorithm. One of the most important effects is due to ρ . If ρ has a high value which means higher channel resolution, MP algorithm can detect tap positions closer to the exact tap delay locations. However, it increases computational complexity as it needs ρ times more computation. Despite the challenges and complexity, MP algorithm is suitable for practical implementation because it jointly estimates all channel parameters.

In Fig. 3.2, a 3-path wireless channel and the MP based estimation are shown in

one snapshot for TVHT-MODE-2C and TVHT-MODE-2N. Also, frequency response of real channel and estimated channels are illustrated. Although MP estimates tap coefficients very closely, there are some incorrect estimated paths which affect the system performance. For this figure, resolution factor ρ is chosen 8, and guard interval rate is chosen $1/8$.

3.5. Performance Measures

To measure symbol error rate (SER) performance, the soft data symbols can be obtained with LMMSE equalizer after estimated delay tap locations and tap coefficients with MP algorithm or the prior knowledge at the nearest integer multiple of T_s/ρ tap delay position and estimated tap coefficients with LMMSE algorithm.

Accordingly, after estimating the channel with either LMMSE or MP based algorithms, estimated channel can be represented as $\widehat{H}[k] = \sum_{\ell=0}^{L-1} \hat{\alpha}_\ell e^{-j \frac{2\pi k}{\rho N} \eta_\ell}$. Then the soft data symbols can be recovered as

$$\begin{aligned} \hat{d}_m[k] &= \frac{E(d[k] Y_m^*[k] | H[k] = \widehat{H}[k])}{E(|Y_m^*[k]|^2 | H[k] = \widehat{H}[k])} \\ &= \frac{\widehat{H}^*[k]}{|\widehat{H}[k]|^2 + N_0} Y_m[k], \end{aligned} \quad (3.15)$$

where $E\{\cdot\}$ is the expectation operator and $(\cdot)^*$ denotes the complex conjugate operator. Since $d_m[k]$ is discrete, $\hat{d}_m[k]$ is assigned to the nearest constellation point and SER performance is calculated.

Average mean-square error (MSE) of channel estimation is calculated in frequency domain due to sparsity of the channel.

The average MSE is calculated as

$$MSE = \frac{1}{K} \sum_{-K/2}^{K/2-1} E\{(H[k] - \widehat{H[k]})^2\} \quad (3.16)$$

where $\widehat{H[k]}$ is estimated channel vector and $H[k]$ is the real channel vector. Expectation is calculated using Monte Carlo simulations.

In the next chapter, system performances of both LMMSE-based and MP-based algorithms are presented and compared.

4. SIMULATION RESULTS

In this chapter, the performance of the MP-based algorithm is assessed and compared with the near-optimal LMMSE approach in terms of different system parameters. In Table 4.1, simulation parameters are given for both TVHT-MODE-2C and TVHT-MODE-2N operation modes. Accordingly, three different modulations BPSK, QPSK and 16QAM are used for computer simulations. Number of empty BCUs are chosen $\{0, 2, 4, 6\}$ respectively where $\{0\}$ empty BCU represents TVHT-MODE-2C. Also, standard defines guard interval rates as $\{\frac{1}{4}, \frac{1}{8}\}$. However $\{\frac{1}{16}\}$ is defined as an optional guard interval rate in this work for investigation. Resolution factor, ρ , is not defined in the standard, but ρ is defined in this work for channel quantization and it directly affects channel estimation performance of the system. Mathematical model of the system is defined in next section.

Constellation type	BPSK, QPSK, 16QAM
Number of empty BCU's	$\{0, 2, 4, 6\}$
Channel bandwidth per BCU (BW)	6 MHz
Number of subcarriers per OFDM symbol (N)	144
Number of active subcarriers per OFDM symbol (K)	128
Subcarrier spacing (Δf)	$41\frac{2}{3}$ KHz
Guard interval rate	$\{\frac{1}{4}, \frac{1}{8}, \frac{1}{16}\}$
Number of pilot symbol per OFDM symbol	6
Resolution Factor (ρ)	$\{1, 2, 4, 8\}$

Table 4.1. Simulation parameters for mode TVHT-MODE-2C and TVHT-MODE-2N

In this chapter firstly, average MSE performance results are presented for TVHT-MODE-2C in different scenarios (different resolution, path numbers, guard interval rates), and TVHT-MODE-2C and TVHT-MODE-2N operation modes are compared when TVHT-MODE-2N has different BCU's in-between. Secondly, symbol error rate

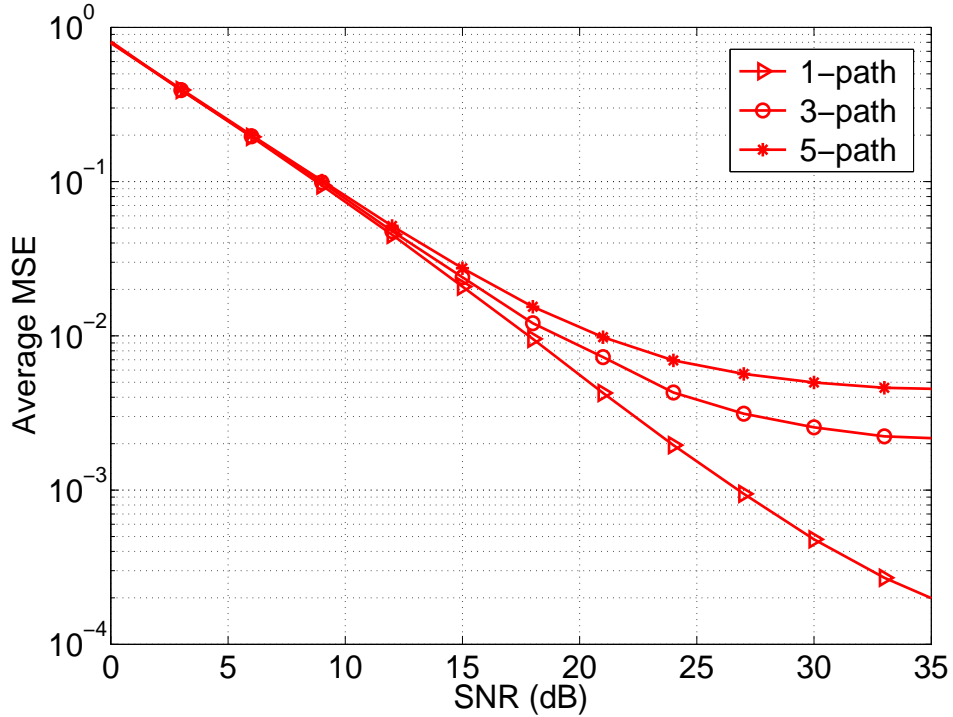


Figure 4.1. Average MSE performances in TVHT-MODE-2C for different number of paths when $\rho=8$, GI rate= $\frac{1}{8}$

performances are compared for LMMSE and MP algorithms in different channel resolutions, which can give idea about performance of practical implementation of the system.

In Fig. 4.1, the effect of number of paths on the MSE performance is presented for the MP algorithm. Resolution effect, ρ , and guard interval rate are fixed to 8 and $\frac{1}{8}$ respectively. $\{1, 3, 5\}$ are selected as numbers of paths. It can be seen that there is no performance difference in the low SNR region due to domination of noise level. The comparison of MSE performances in medium and high SNR regions shows us if number of paths decreases, MSE performance increases. This improvement can be explained with number of pilot tones and estimation of delay tap positions. Channels with less number of paths can be better estimated with same pilot symbols, however, more pilots are needed for estimating more number of paths.

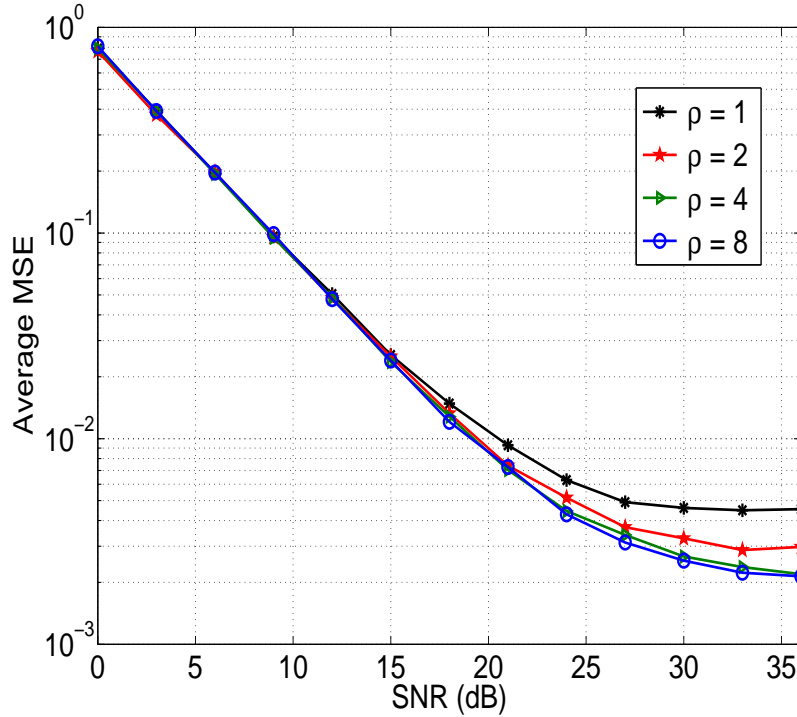


Figure 4.2. Average MSE performances in TVHT-MODE-2C for different channel resolutions when 3-path wireless channel and GI rate= $\frac{1}{8}$ are used

Fig. 4.2 presents MSE performances for different ρ values in TVHT-MODE-2C operation mode. QPSK is used as the modulation type, channel has 3 paths and short guard interval rate (i.e., $\frac{1}{8}$) is chosen from IEEE 802.11af standard. $\{1,2,4,8\}$ are selected as ρ values for investigating channel resolution effect. Higher ρ values provide better channel resolution, which helps MP algorithm to estimate delay positions. It can be seen that until a stopping condition, there is slight performance improvement of MSE performances, but after a certain SNR, MSE performance remains constant. Furthermore, $\rho = 4$ and $\rho = 8$ perform similar.

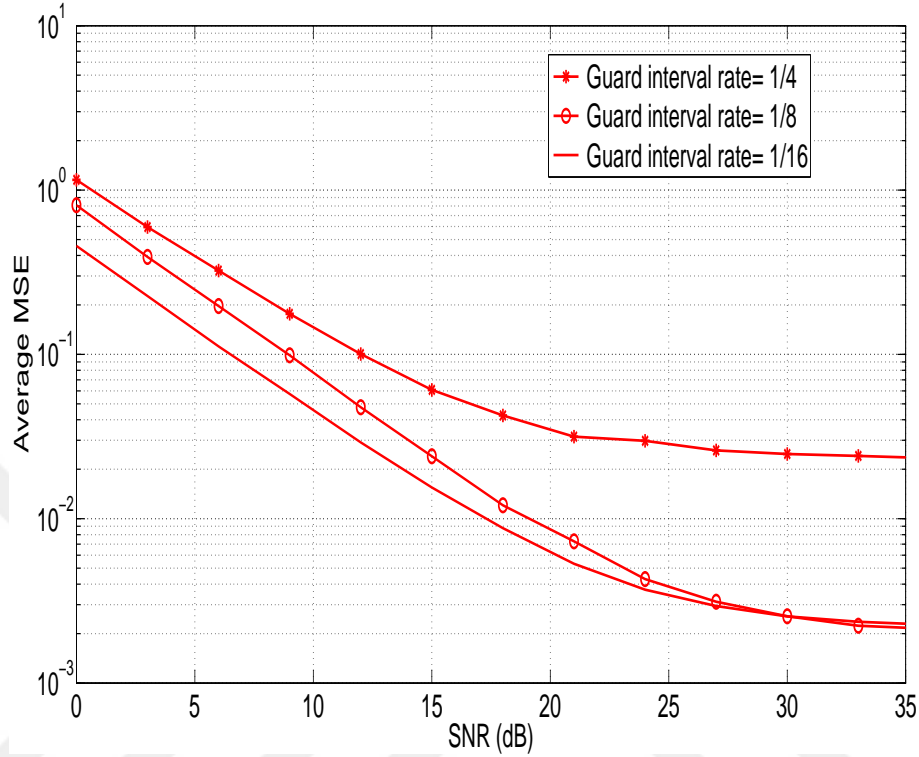


Figure 4.3. Average MSE performances of TVHT-MODE-2C for various guard interval rates when 3-path wireless channel is considered

Fig. 4.3 presents average MSE performance for different guard interval rates of TVHT-MODE-2C operation mode. Channel is selected to contain 3 paths, ρ is chosen 8 and modulation type is QPSK. $\{\frac{1}{4}, \frac{1}{8}\}$ are provided as regular guard interval rate and short guard interval rate, respectively, in IEEE 802.11.af standard. $\{\frac{1}{16}\}$ is selected as an optional guard interval rate in this study. It can be seen that when guard interval rate drops from $\frac{1}{4}$ to $\frac{1}{8}$, MSE performance improves significantly. On the other hand, MSE performance remains constant for $\frac{1}{8}$ and $\frac{1}{16}$ guard interval rates in the high SNR region. Hence, decreasing the guard interval rate, MSE performance will not improve anymore. In addition, short guard intervals can be suggested for practical implementation.

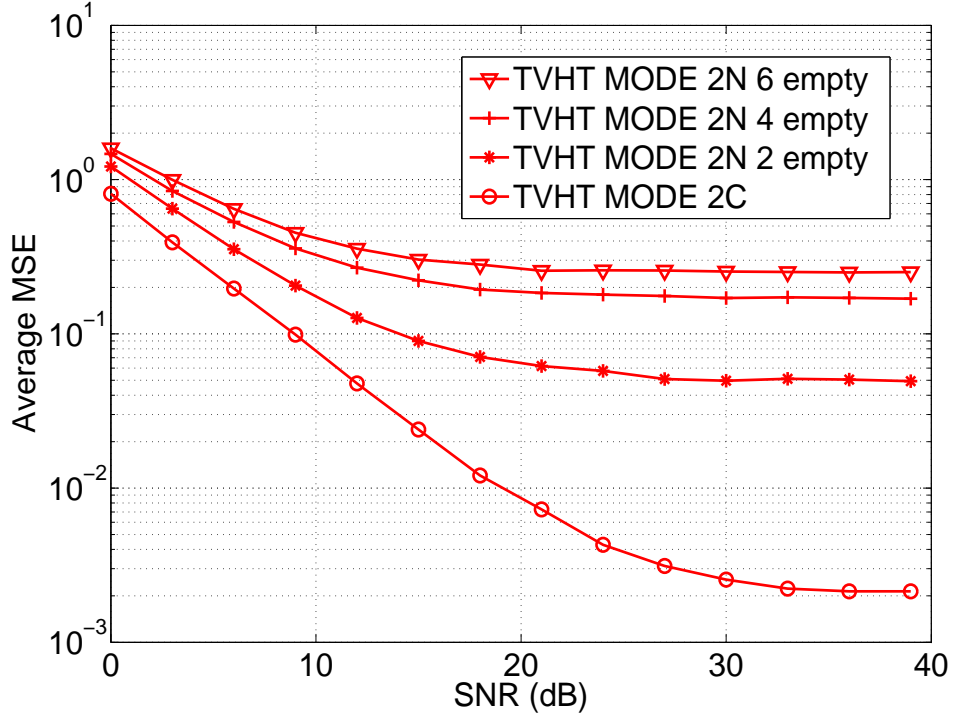


Figure 4.4. Average MSE performances in different operation modes when 3-path wireless channel, GI rate= $\frac{1}{8}$ and $\rho = 8$ are used

In Fig. 4.4, MSE performances of TVHT-MODE-2C and TVHT-MODE-2N are compared for $\{2,4,6\}$ in-between empty BCU's for QPSK modulation in 3-path channel. The resolution effect, $\rho = 8$, and guard interval rate is $\frac{1}{8}$, which is the short guard interval for TVHT operation mode. Channel tap delay positions and tap delay coefficients are estimated by the MP algorithm. It can be seen clearly that, MSE performance becomes worse due to increasing interpolation errors of channel estimation when the number of BCU's in-between is increased. OFDM pilot symbols cannot interpolate well due to the distances in-between bands and hence, TVHT-MODE-2N performs inferior when MP algorithm is employed.

Fig. 4.5 presents the SER performance comparison of MP algorithm and LMMSE approach with rounding delay positions. BPSK, QPSK and 16QAM are used as modulation types, short guard interval rate $\frac{1}{8}$ is chosen and the channel has 3 paths. Delay positions are rounded to the closest interval and ρ is selected 1. It can be seen that MP algorithm starts to perform better after 20 dB SNR for every modulation type. This is due to MP algorithm performing better when high rounding errors happen.

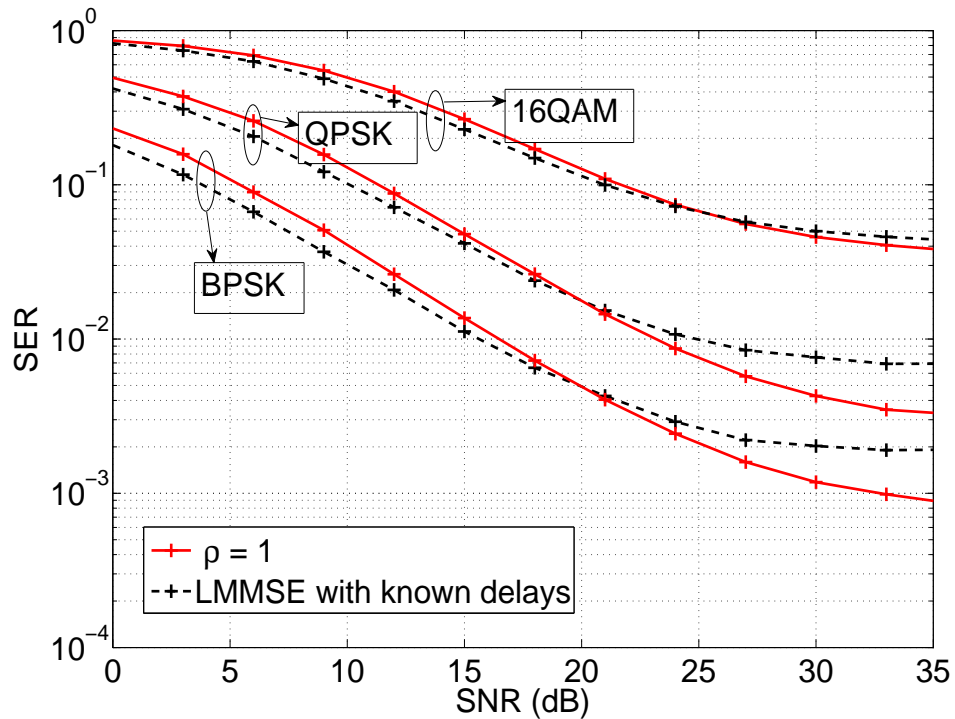


Figure 4.5. SER comparison of MP algorithm and LMMSE estimation when channel resolution $\rho = 1$, 3-path wireless channel, GI rate= $\frac{1}{8}$ are used

Fig. 4.6 shows the SER performance comparison of MP algorithm and LMMSE approach with rounding delay positions, when the delay positions are rounded to the closest interval and ρ is selected 4. MP algorithm performance is close to rounding performances for every modulation type but it can not perform better because the rounding error is minimized. On the other hand, MP algorithm may reach the same performance as the rounding case in high channel resolutions if number of pilot tones are increased.

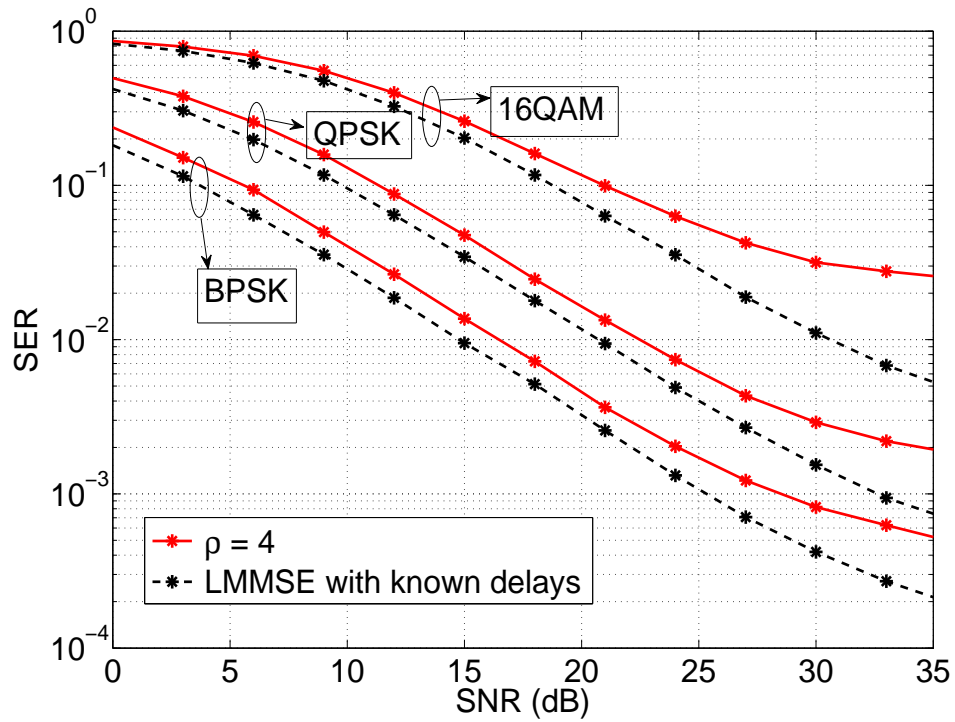


Figure 4.6. SER comparison of MP algorithm and LMMSE estimation when channel resolution $\rho = 4$, 3-path wireless channel, GI rate= $\frac{1}{8}$ are used

Finally, in Fig. 4.7, the SER performance comparison of MP algorithm and LMMSE approach are compared when $\rho = 8$. In addition, in order to show that LMMSE with delay known is close to optimal, perfectly known coefficients and delays (rounded) is plotted for comparison. It can be that LMMSE is only about 0.5 – 1 dB inferior to knowing the magnitude case. On the other hand, MP performance does not improve much when ρ is increased from 4 to 8. This was also observed in Fig. 4.2. All in all, the MP algorithm is only 1 – 2 dB inferior to the near-optimal LMMSE with in the low and medium SNR region, where communication occurs in practice.

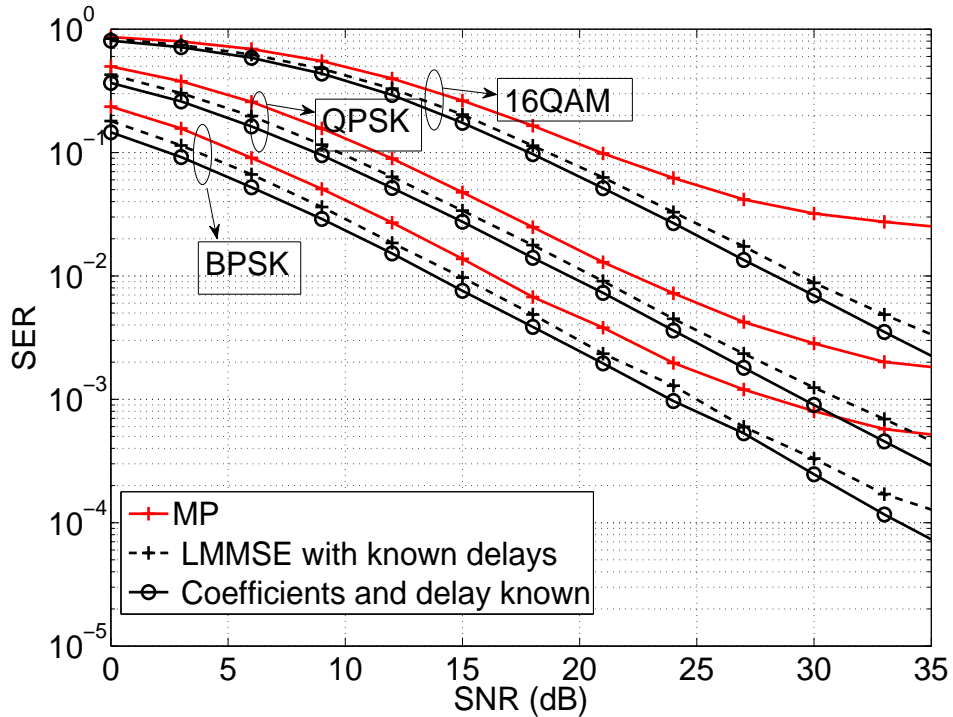


Figure 4.7. MP algorithm and rounding on LMMSE estimation comparison in channel resolution $\rho = 8$, 3 path wireless channel, GI rate= $\frac{1}{8}$.

5. CONCLUSIONS and FUTURE RESEARCH

5.1. Conclusions

In this thesis, the practical implementation of the WLAN standard in TVWS, i.e., IEEE 802.11af standard, is considered under realistic channel conditions. Since the number of pilot tones allowed in the standard is very low, a sparse multipath channel model is used in order to decrease the unknown channel parameters resulting in a better channel estimation performance. In order to increase the transmission bandwidth, the standard allows the use of non-contiguous BCUs. This separation between OFDM symbols and a low resolution of the discrete-time equivalent multipath channel may have negative effects on the overall system performance. In this study, the effects of channel resolution, guard interval rate, number of paths and the separation between BCUs in contiguous and non-contiguous mode were investigated for the IEEE 802.11af systems under various practical scenarios.

The following observations are made:

- As the number of in-between-bands occupying the non-contiguous modes is increased the channel estimation performance degrades drastically.
- When the guard interval rate is decreased from $1/4$ to $\{1/8, 1/16\}$, there is significant improvement on the channel estimation performance.
- When the selected channel resolution is increased, the channel estimation performance improves. For the selected parameters, $\rho = 4$ is found to be a sufficient value.
- MP-based channel estimation performance is only 1-2 dB inferior compared to LMMSE-based estimation with known delays in low and medium SNR regions.

In addition, it is shown that there is only slight performance difference between knowing both delay locations and magnitudes and knowing only delay locations and estimating the magnitudes.

5.2. Future Research

There are several issues that can be addressed in future research of this study to improve system performances.

- Pilot tone locations are not defined as equally-spaced in the IEEE 802.11af standard. Investigating pilot tone placing may be a subject for the future research.
- Frequency selective fading channels can be considered for the simulations, instead of static channel.
- Matching Pursuit algorithm is implemented for practical estimation as an example. Instead of MP, orthogonal matching pursuit algorithm can be implemented for estimating delay locations and magnitudes.
- Finally, system performances are investigated theoretically in this work. The studied approaches can be implemented on real systems to test performances.

REFERENCES

1. M.Z. Win and R.A. Scholtz, "Ultra-wide bandwidth time-hopping spread spectrum impulse radio for wireless multiple-access communications ", IEEE Trans Commun., vol. 48, pp. 679691, 2000.
2. J. Mitola and G.Q. Maguire, "Cognitive radio: making software radios more personal," IEEE Personal Commun., vol. 6, pp. 13-18, 1999.
3. S. Bayhan ve F. Alagöz, "TV beyaz spektrum iletişimi: temel bilgiler ve güncel gelişmeler", Proc. Akademik Bilişim Konferansı, Şubat 2011.
4. C.-S. Sum et. al., "Cognitive communication in TV white spaces: an overview of regulations, standards, and technology", IEEE Commun. Mag., pp. 138 - 145, July 2013.
5. J. Markendahl, P. Gonzales-Sanchez, and B. Mlleryd, "Impact of deployment costs and spectrum prices on the business viability of mobile broadband using TV white space", Proc. ICTS-CROWNCOM-2012, pp. 124-128.
6. M. Fitch, M. Nekovee, S. Kawade, and R. MacKenzie, "Wireless service provision in TV white space with cognitive radio technology: a telecom operators perspective and experience", IEEE Commun. Mag., pp. 64 - 73, Mar 2011.
7. IEEE 802.22, Enabling Broadband Wireless Access Using Cognitive Radio Technology and Spectrum Sharing in White Spaces, 2011.
8. IEEE 802.15.4m, TV White Space Amendment to IEEE 802.15.4, 2014.
9. IEEE Std 802.11af, IEEE Standard for information technology – Telecommunications and information exchange between systems - Local and metropolitan area networks - Specific requirements - Part 11: Wireless LAN Medium Access Control

- (MAC) and Physical Layer (PHY) Specifications Amendment 5: Television White Spaces (TVWS) Operation, 2013.
10. C.-S. Sum et. al., "IEEE 802.15.4m: the first low rate personal area networks operating in TV white space", Proc. ICON-2012, pp. 326 - 331.
 11. C.-S. Sum et. al., "Design considerations of IEEE 802.15.4m low-rate WPAN in TV white space", IEEE Commun. Mag., pp. 74 - 82, Apr. 2013.
 12. IEEE 802.19.1, Wireless Coexistence in TV White Space, 2014.
 13. K. Harrison, S. M. Mishra, and A. Sahai, "How much white-space capacity is there?", Proc. DySPAN- 2010.
 14. J. Beek, J. Riihijarvi, A. Achtzehn, and P. Mahnen, "TV white space in Europe, IEEE Trans. Mobile Computing", vol. 11, pp. 178 - 188, Feb. 2012.
 15. J. Beek, J. Riihijarvi, A. Achtzehn, and P. Mahnen, "UHF white space in Europe a quantitative study into the potential of the 470-790 MHz band", Proc. DySPAN-2011.
 16. H.-S. Chen and W. Gao, "Spectrum sensing for TV white space in North America", IEEE Jour. Selec. Areas Commun., vol. 29, pp. 316- 326, Feb. 2011.
 17. A. Achtzehn et. al., "Improving coverage prediction for primary multi-transmitter networks operating in the TV whitespaces", Proc. SECON-2012, pp. 547 - 555.
 18. L. Simic, M. Petrova, and P. Mahnen, "Wi-Fi, but not on steroids: performance analysis of a wi-fi-like network operating in TVWS under realistic conditions", Proc. IEEE ICC-2012, pp. 1533 - 1538.
 19. X. Chen and J. Huang, "Database-assisted distributed spectrum sensing", IEEE Jour. Selec. Areas Commun., vol. 31, Nov. 2013.

20. J.-S. Um, S.-H. Hwang, and B. J. Jeong, "A comparison of PHY layer on the Ecma-392 and IEEE 802.11af standards", Proc. CROWNCOM-2012, pp. 315 - 319.
21. J. Heo et. al., "Mobile TV white space with multi-region based mobility procedure", IEEE Wireless Commun. Lett., vol. 1, pp. 569 - 572, Dec. 2012.
22. T. Bansal, D. Li, and P. Sinha, "Opportunistic channel sharing in cognitive radio networks", IEEE Trans. Mobile Computing, vol. 13, pp. 852- 865, Apr. 2014.
23. A. Achtzehn, M. Petrova, and P. Mahnen, "On the performance of cellular network deployments in TV whitespaces", Proc. IEEE ICC-2012, pp. 1814 - 1819.
24. C. Song et. al., "Autonomous dynamic frequency selection for WLAN operating in the TV white space", Proc. IEEE ICC-2011.
25. T. Baykas. Et. al., "Developing a standard for TV white space coexistence: technical challenges and solution approaches", IEEE Wireless Commun., pp. 10 - 22, Feb. 2012.
26. S. Filin, T. Baykas, M. A. Rahman, and H. Harada, "Performance evaluation of IEEE 802.19.1 coexistence system", Proc. IEEE ICC-2011.
27. G. P. Villardi et. al., "Enabling coexistence of multiple cognitive networks in TV white space", IEEE Wireless Commun., pp. 32 - 40, Aug. 2011.
28. J. Huang, G. Xing, G. Zhou, and R. Zhou, "Beyond co-existence: exploiting WiFi white space for ZigBee performance assurance", Proc. ICNP-2010, pp. 305 - 314.
29. J.-J. Deslie "Whats the Difference between IEEE 802.11af and 802.11ah?", MICROWAVES & RF, pp. 69-72, April 2015.
30. Federal Communications Commission, Third Memorandum and Order, Apr. 2012.

31. Z. Lan, K. Mizutani, G. Villardi, and H. Harada, "Design and implementation of a Wi-Fi prototype system in TVWS based on IEEE 802.11af," *Proc. IEEE WCNC*, pp. 750–755, Apr. 2013.
32. Z. Lin, M. Ghosh, and A. Demir, "A comparison of MAC aggregation vs. PHY bonding for WLANs in TV white spaces," *Proc. IEEE PIMRC*, pp. 1829–1834, Sep. 2013.
33. L. Simic, M. Petrova, and P. Mahonen, "Wi-Fi, but not on steroids: performance analysis of a Wi-Fi like network operating in TVWS under realistic conditions," *Proc. IEEE ICC*, pp. 1533–1538, Jun. 2012.
34. C.-S. Sum, M.-T. Zhou, L. Lu, F. Kojima, and H. Harada, "Performance and coexistence analysis of multiple IEEE 802 WPAN/WLAN/WRAN systems operating in TV white space," *Proc. IEEE DySPAN*, pp. 145–148, Apr. 2014.
35. J.-S. Um, S.-H. Hwang, and B.J. Jeong, "A comparison of PHY layer on the Ecma-392 and IEEE 802.11af standards," *Proc. ICST CROWNCOM*, pp. 315–319, Jun. 2012.
36. K. Mizutani, Z. Lan, R. Funada, and H. Harada, "IEEE 802.11af with partial subcarrier system for effective use of TV white spaces," *Proc. IEEE ICC*, pp. 1255–1259, Jun. 2013.
37. C.R. Berger, S. Zhou, J. Preisig, and P. Willett, "Sparse channel estimation for multicarrier underwater acoustic communication: from subspace methods to compressed sensing," *IEEE Tran. Signal Process.*, vol. 58, pp. 1708–1721, Mar. 2010.
38. Habib Senol, "Joint channel estimation and symbol detection for OFDM systems in rapidly time-varying sparse multipath channels," *Wireless Personal Communications*, vol. 82, issue 3, pp. 1161–1178, June 2015.
39. M. C. Macit, H. Şenol, S. Erküçük "Performance investigation of IEEE802.11af

under realistic channel conditions.” *IEEE IWCMC*, pp. 431–435, Aug. 2015



APPENDIX A: APPENDIX

A.1. *

Curriculum Vitae

Mustafa Can Macit was born on 17 May 1991 in Ankara. He received his B.Sc degree in Electronics Engineering in 2013 from Kadir Has University. He worked as a research assistant and a teaching assistant at the Department of Electronics Engineering of Kadir Has University from 2013 to 2016. His research interests are in the design of emerging communication systems and wireless sensor networks.

Publications:

[1] S. Baktr, A. Ozmen, T. Gucluoglu, H. F. Alsan, M.C. Macit, “Detection of Trojans in Integrated Circuits”, International Symposium on Innovations in Intelligent Systems and Applications(INISTA), Trabzon, July 2012

[2] M. C. Macit, H. Şenol, S. Erküçük “Performance investigation of IEEE802.11af under realistic channel conditions,” *IEEE IWCMC*, pp. 431–435, Aug. 2015